Estonian Journal of Engineering, 2012, **18**, 3, 279–287 doi: 10.3176/eng.2012.3.13

Visualization of strain distribution around the edges of a rectangular foreign object inside the woven carbon fibre specimen

Henrik Herranen[a], Georg Allikas[b], Martin Eerme[a], Karl Vene[a], Tauno Otto[a], Andre Gregor[b], Maarjus Kirs[a] and Karl Mädamürk[c]

[a] Department of Machinery, Tallinn University of Technology, Ehitajate tee 5, 19086 Tallinn, Estonia; henrik.herranen@ttu.ee
[b] Department of Materials Engineering, Tallinn University of Technology, Ehitajate tee 5, 19086 Tallinn, Estonia
[c] Department of Computer Control, Tallinn University of Technology, Ehitajate tee 5, 19086 Tallinn, Estonia

Received 19 June 2012, in reveised form 23 July 2012

Abstract. The paper addresses the issue of embedding the rectangular printed circuit board (PCB) – the placeholder for a complex sensor system circuit – in the glass fibre laminate during the lamination. The change of the material mechanical properties due to the presence of foreign objects in the laminate is assessed by experimental testing through standardized methods ASTM D3039, ASTM D6641 and ASTM D3518. Local stress–strain relationship near the PCB in the out-of-plane direction of the specimen are monitored through the use of GOM ARAMIS 2M digital image correlation method scanner. Based on the scanned model, a finite element simulation is generated and validated.

Key words: composite, laminate embedded printed circuit board, carbon fibre, digital image correlation.

1. INTRODUCTION

Surface-mounted sensors are susceptible to damage and their protection form environment is often accompanied by noticeable extra weight increase. Embedding the sensors allows for protection from adverse environmental conditions. If high environment protection enclosures like IP67 are removed, a noticeable weight saving occurs. It is also the only means suitable for creating an autonomous structure with a smooth surface finish.

Estimation of the structure behaviour in the case when a simple geometry sensor is embedded in the host structure, has been analysed earlier [1–6]. In [1], a field effect transistor is embedded in a structure and is tested to electronics functionality failure. Main difference from the current article is the simplicity of the circuit and that the laminas have inclusions. In [2], limited tests (3-point bending and compression) with embedded sensors are conducted. Paper [3] describes the performance of a laminate with embedded sensors, which interface to host structure is reinforced with interlacing. Papers [5] and [6] handle the mechanical behaviour of a laminate with simple piezoelectric actuators.

This article describes the mechanical issues, related to embedding naked electronics circuits of complex geometry inside a carbon fibre composite. A finite element model is generated. It is validated through strain field comparison with the results of digital image correlation scanner GOM ARAMIS 2M.

2. EXPERIMENTAL SET-UP AND RESULTS

The base material is GURIT supplied carbon fibre woven pre-preg fabric with designation SE84 LV. The material was cured under 1 bar vacuum in an oven at around 80 °C according to the supplier provided curing cycle. The fabric has surface density of 200 g/m^2. The number of lamina layers in the laminate is 16. The thickness of the laminate is 3.5 mm.

Host material was tested for in-plane properties only. Tensile testing was conducted according to ISO 527-4, shear testing according to ASTM D3518 and compression testing according to ASTM 6641. All three tests were conducted by using 10 identical specimens.

The virgin carbon fibre structure has in-plane properties as stated in Table 1. Directions x and y are equivalent.

For the electronics placeholder, an available printed circuit board with low thickness and casingless microchips was chosen. The PCB is depicted in Fig. 1. It is 22 mm long and 15 mm wide. The height of the board is 0.6 mm. The thickness at the widest section is 2.45 mm.

The circuit board was embedded in 5 specimens with orientation as shown in Fig. 2.

Table 1. Mechanical properties of the host laminate virgin structure

Property	Value	Unit
Tensile strength, $\sigma^t_x = \sigma^t_y$	625.65 ± 39.8	MPa
Maximum tensile strain, $\varepsilon^t_x = \varepsilon^t_y$	0.987 ± 0.188	%
Compressive strength, $\sigma^c_x = \sigma^c_y$	347 ± 16	MPa
Maximum compressive strain, $\varepsilon^c_x = \varepsilon^c_y$	0.49 ± 0.097	%
Youngs modulus, $E_x = E_y$	57.88 ± 28.2	GPa
Shear strength, τ_{xy}	92.27 ± 4.74	MPa
Maximum shear strain, γ_{xy}	4.74 ± 0.456	%
Shear modulus, G_{xy}	7.065 ± 1.73	GPa

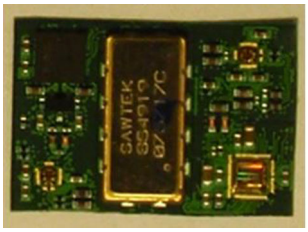

Fig. 1. Embedded electronics circuit.

Fig. 2. Orientation of the embedded circuit.

Chips were placed between the 8th and the 9th layer to ensure that they were on the neutral axis. Dipping the PCB-s inside acetone to remove any traces of dirt or grease was the only pre-treatment that was done before the lamination process. The material was fabricated on a glass plate to imitate a production mould that ensures a smooth continuous surface on one side. This formed a structure that has asymmetry in the *z* direction.

The specimens with embedded electronics were tested to failure with tensile, compressive and shear loads. The results are summarized in Table 2.

Compressive properties of the material were most affected: compressive strength was reduced by 31.5% and compressive strain by 66.8%

Table 2. Mechanical properties of the specimens with electronics

Property	Value	Unit	Change compared to virgin structure, %
Tensile strength, $\sigma^t_x = \sigma^t_y$	490.66 ± 48.08	MPa	–21.6
Maximum tensile strain, $\varepsilon^t_x = \varepsilon^t_y$	1.186 ± 0.12	%	16.8
Compressive strength, $\sigma^c_x = \sigma^c_y$	237.73 ± 18.76	MPa	–31.5
Maximum compressive strain, $\varepsilon^c_x = \varepsilon^c_y$	0.491 ± 0.149	%	–66.8
Shear strength, τ_{xy}	85.58 ± 11.4	MPa	–7.3
Maximum shear strain, γ_{xy}	4.25 ± 1.11	%	–10.3

3. FINITE ELEMENT MODEL

A 2D plane stress finite element model is constructed using software ANSYS V14.0. The CAD geometry was directly derived from pictures of the microscope (Figs 3 and 4). The scale was determined based on the microscope scale ruler on the original pictures and was double-checked, based on the measurements made earlier on the electronics board (length, width, thickness of the PCB board, height of the surface acoustic wave device). Simulation model mesh is depicted in Fig. 5. It has 32 032 elements.

In the cross-section of the PCB, the most space consuming parts are the surface acoustic wave (SAW) filter and the circuit board. The SAW device consists of two materials: steel cap and quartz wafer onto which the filter circuit is etched. The mechanical properties of used materials are listed in Table 3. The properties of electronics are derived from literature. The printed circuit board is composed of copper layers and of glassfibre/epoxy composite FR-4. FR-4 properties are taken from [7,8]. Quartz and copper are both taken from [1].

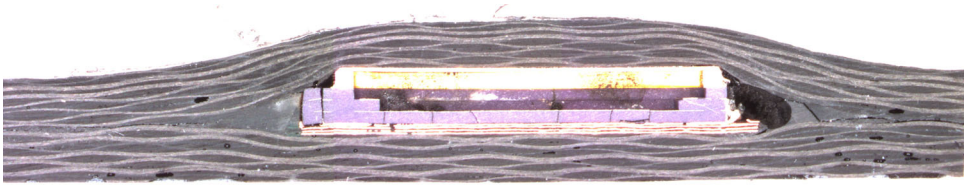

Fig. 3. Cross-sectional view of the specimen after failure.

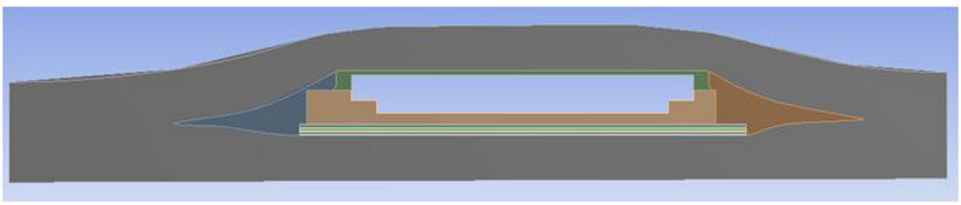

Fig. 4. Constructed finite element model.

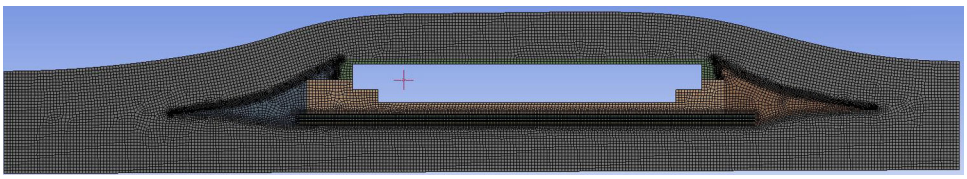

Fig. 5. The mesh of the model had 32 032 elements with refinements at the edges of the interfaces of the materials.

Table 3. Mechanical properties of materials used in simulation

Material	Material model	Elasticity properties	Strength properties
Quartz	Isotropic, linear	E = 7 GPa, ν = 0.17	σ_t = 100 MPa, σ_c = 1100 MPa
Steel	Isotropic, bilinear kinematic hardening	E = 200 GPa, ν = 0.3, $E_{tangent}$ = 40 GPa	σ_{yield} = 250 MPa, σ_u = 510 MPa
Copper	Isotropic, bilinear kinematic hardening	E = 130 GPa, ν = 0.34, $E_{tangent}$ = 25 GPa	σ_y = 45 MPa, σ_u = 210 MPa
FR-4 glassfibre laminate	Isotropic, linear	E = 20 GPa, ν = 0.20	σ_t = 345 MPa, σ_c = 415 MPa
Epoxy resin	Isotropic, linear	E = 3.8 GPa, ν = 0.4	σ_t = 98 MPa, σ_c = 172 MPa

The only anisotropic material in the finite element model is the carbon fibre laminate with orthotropic properties as measured on the virgin structure, mentioned in Table 1.

Virtual model of the specimen cross-section was loaded with 0.6% strain. At this strain level a loud cracking sound occurred, which indicates the structural failure of some embedded circuit board components. At this point the average stress in the tensile specimen is 353 MPa. Simulation results are depicted in Figs 6 and 7. The stress distribution in the cross-section of the specimen is shown in Fig. 6. Highest stress levels occur at the edges of the steel cap and under the printed circuit board. From these points the failure is initiated.

The factor of safety for materials, based on their ultimate strength, is plotted in Fig. 7. The lowest values are at the edges of the steel cap, quartz wafer and ends of PCB. Therefore the lowest strength in this application occurs in the region where the high-stiffness steel cap is adhered to the carbon fibre laminate.

4. VALIDATION OF THE FINITE ELEMENT MODEL

The finite element model is validated through the comparison with digital image correlation scanner results. The surface strains of the specimens were measured with a digital image correlation system (DIC) GOM ARAMIS 2M. The measuring volume was set to 35×25 mm. Project parameters are as follows: the computational size is set to 3, validity quote 55%, the calculation method is set to total strain method and computation type is set to plane stress. Scanner data is taken from the stage, where tensile strain is 0.6% (equals to 32080 N tensile force and 353 MPa tensile stress). The tensile strain distribution on the curved surface of the specimen is depicted in Fig. 8.

The FEM top surface strain distribution is compared with the DIC scanner data in Fig. 9. The curves of strain distributions are close to each other, with strain difference 0.35% at the even surface (between longitudinal coordinates 10 to 20 mm). In physical specimens the tensile strains are higher up to 1.0%.

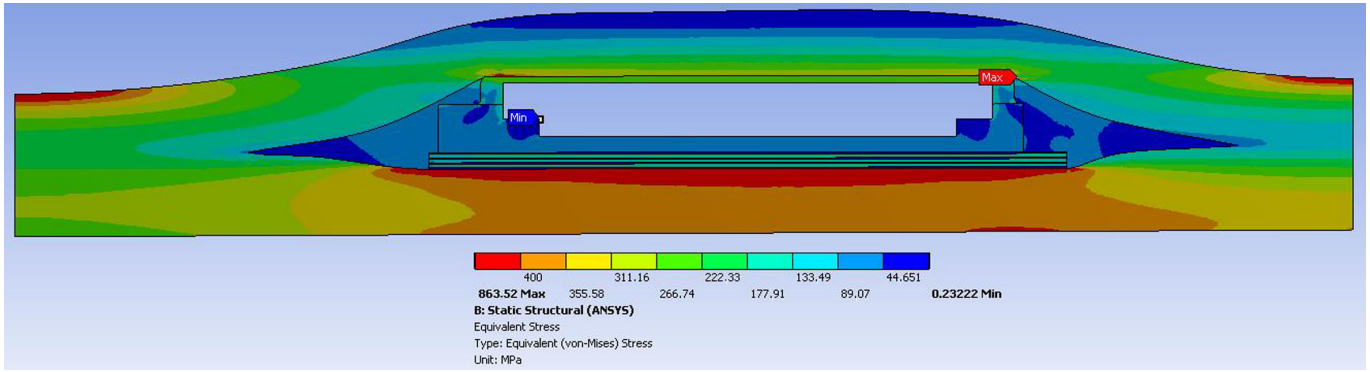

Fig. 6. Von Mises stress distribution in the specimen.

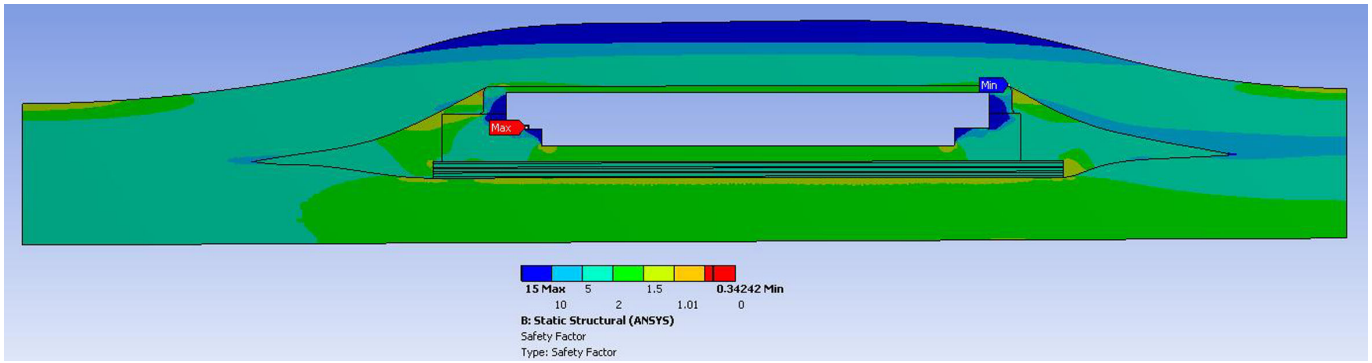

Fig. 7. Factor of safety of the materials.

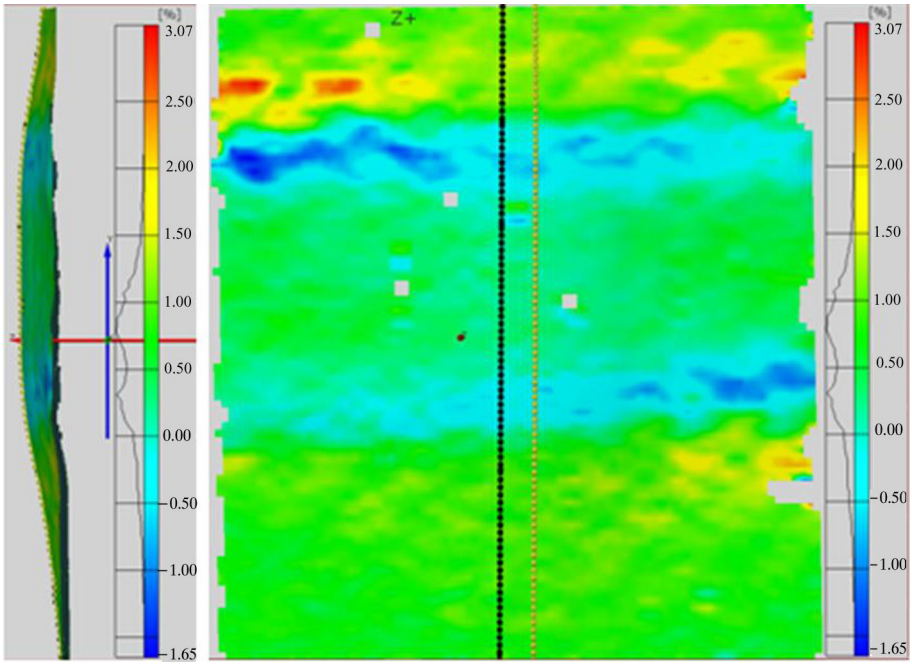

Fig. 8. Tensile strain distribution on the surface of the transversely placed PCB specimen, measured with the digital image correlation scanner. The black vertical line shows the location of the section where the strain is compared with the FEM model results.

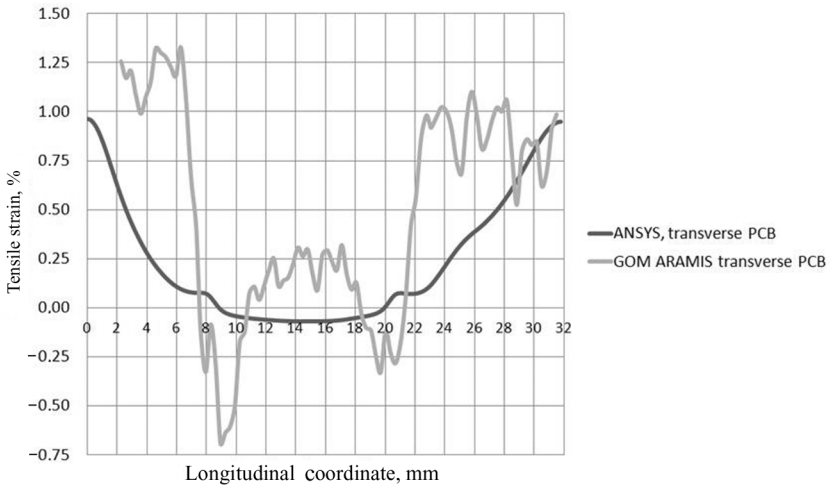

Fig. 9. Comparison of the tensile strain distributions.

This can be explained by the impurities, located at the edges of the SAW device. One such example is seen in Fig. 3 as a void or air bubble at the edge of the steel

cap. Waviness of the DIC measured strain distribution is probably caused by the weaving pattern of the fabric. The FEM model uses homogenized material for the composite laminate, which has much more smoother strain distribution.

5. CONCLUSIONS

A finite element method simulation was made in order to investigate the inner stresses of a composite structure with embedded electronics. The simulation was validated with tensile strain data from experimental testing. The strain distribution shows good correlation, which is influenced strongly by the impurities of the real material. Failure of the whole structure starts from the mismatch of the stiffness properties between steel and the composite material. This creates stress concentration that reduces the mechanical properties of the host material up to 32% of ultimate compressive strength. Future research direction would be the development of a suitable casing and multicriteria optimization procedure, like in [9,10] for optimizing the host structure and electronics to smoothen the stress gradients. The interaction between the host structure and the electronics can be influenced by multiple variables such as thickness of the electronics, thickness of the laminate, orientation of the laminas, geometrical shape of the electronics, etc.

REFERENCES

1. Warkentin, D. J. and Crawley, E. F. Embedded electronics for intelligent structures. In *Proc. AIAA 32nd Conference on Structures, Structural Dymanics and Materials*. Baltimore, 1991. AIAA Paper, AIAA-91-1084CP, 1991, 1322–1331.
2. Kim, K. S., Breslauer, M. and Springer, G. S. The effect of embedded sensors on the strength of composite laminates. *J. Reinforced Plastics Composites*, 1992, **11**, 949–958.
3. Sirkis, J. S., Singh, H., Dasgupta, A. and Chang, C. C. Experimental determination of damage and interaction strain fields near active and passive inclusions embedded in laminated composite materials. In *Proc. ADPA/AIAA/ASME/SPIE Conference on Active Materials and Adaptive Structures*. Alexandria, USA, 1992, 563–566.
4. Hansen, J. P. and Vizzini, A. J. Fatigue response of a host structure with interlaced embedded devices. *J. Intelligent Mater. Syst. Struct.*, 2000, **11**, 902–909.
5. Mall, S. and Coleman, J. M. Monotonic and fatigue loading behavior of quasi-isotropic graphite/epoxy laminate embedded with piezoelectric sensor. *Smart Mater. Struct.*, 1998, **7**, 822–832.
6. Paget, C. A. and Levin, K. Structural integrity of composites with embedded piezoelectric ceramic transducer. In *Proc. SPIE Conference on Smart Structure and Integrated Systems*. Newport Beach, California, 1999, SPIE 3668, 306–312.
7. Acculam Epoxyglas G10/FR4. *IDES Prospector*. IDES Inc., 2012. http://prospector.ides.com/DataView.aspx?I=34&TAB=DV_DS&E=112876&SKEY=34.986842.50872380%3A9a0ec215-bdfc-41a9-86ea-7110135e126e&CULTURE=en-US
8. Arlon 45N properties. *IDES Prospector*. IDES Inc., 2012. http://prospector.ides.com/DataView.aspx?I=34&TAB=DV_DS&E=120891&SKEY=34.986842.50872380%3A9a0ec215-bdfc-41a9-86ea-7110135e126e&CULTURE=en-US
9. Pohlak, M., Karjust, K. and Küttner, R. Multi-criteria optimization of large composite parts. *Composite Struct.*, 2010, **92**, 2146–2152.

10. Pohlak, M. and Majak, J. Optimal material orientation of linear and non-linear elastic 3D anisotropic materials. *Meccanica*, 2010, **45**, 671–680.

Suhteliste deformatsioonide visualiseerimine süsinikkiudkomposiidis neljakandilise objekti ümbruses

Henrik Herranen, Georg Allikas, Martin Eerme, Karl Vene, Tauno Otto, Andre Gregor, Maarjus Kirs ja Karl Mädamürk

On uuritud pingejaotust süsinikkomposiidist katsekeha ristlõikes, millesse on integreeritud õhuke elektroonika trükkplaat. Pingete kontsentratsiooni analüüsitakse, kasutades lõplike elementide meetodi tarkvara ANSYS V14.0. Simulatsiooni korrektsust kontrollitakse tulemuste võrdlemisega digitaalse pildi korrelatsiooniskanneri GOM ARAMIS 2M abil määratud tõmbedeformatsioonidega. Simulatsioonist selgub, et kõige tugevamini mõjutavad komposiitmaterjali sinna lamineeritud jäigad metalsed kehad. Skaneerimise andmeid mõjutavad kõige enam pooride olemasolu ja süsiniklaminaadi kiududest tingitud mikrotaseme mitteisotroopsus.